Veterinary Microbiology 233 (2019) 147–153

Contents lists available at ScienceDirect

Veterinary Microbiology

journal homepage: www.elsevier.com/locate/vetmic

ATN-161 reduces virus proliferation in PHEV-infected mice by inhibiting the integrin α5β1-FAK signaling pathway

Xiaoling Lv[a,1], Zi Li[a,1], Jiyu Guan[a], Jing Zhang[a], Baofeng Xu[b], Wenqi He[a], Yungang Lan[a], Kui Zhao[a], Huijun Lu[c], Deguang Song[a], Feng Gao[a,*]

[a] Key Laboratory of Zoonosis Research, Ministry of Education, College of Veterinary Medicine, Jilin University, Changchun 130062, China
[b] Department of Neurosurgery, The First Hospital of Jilin University, Changchun, 130021, China
[c] Key Laboratory of Zoonosis Research, Ministry of Education, Institute of Zoonosis, Jilin University, Changchun 130062, China

ARTICLE INFO

Keywords:
Porcine hemagglutinating encephalomyelitis virus
Integrin α5β1
FAK
ATN-161

ABSTRACT

Porcine hemagglutinating encephalomyelitis virus (PHEV) is a typical neurotropic virus that can cause obvious nerve damage. Integrin α5β1 is a transmembrane macromolecular that closely related to neurological function. We recently demonstrated that integrin α5β1 plays a critical role in PHEV invasion in vitro. To determine the function and mechanism of integrin α5β1 in virus proliferation in vivo, we established a mouse model of PHEV infection. Integrin α5β1-FAK signaling pathway was activated in PHEV-infected mice by qPCR, Western blotting, and GST pull-down assays. Viral proliferation and integrin α5β1-FAK signaling pathway were significantly inhibited after intravenous injection of ATN-161, an integrin α5β1 inhibitor. Through a histological analysis, we found that ATN-161-treated mice only showed pathological changes in neuronal cytoplasmic swelling at 5 day post-infection. In summary, our results provide the first evidence that ATN-161 inhibits the proliferation of PHEV in mice and explores its underlying mechanisms of action.

1. Introduction

Porcine hemagglutinating encephalomyelitis (PHE) is an acute and highly contagious disease caused by infection with porcine hemagglutinating encephalomyelitis virus (PHEV), which mainly affects piglets within 3 weeks of age, causing vomiting and wasting disease and/or obvious neurological symptoms (Li et al., 2017a, 2016). PHEV is a member of the family *Coronaviridae*, which can cause susceptible neurological dysfunction in susceptible animals, including pigs, mice, and rats (Shi et al., 2018). In 1962, the virus was first isolated from the brains of infected piglets in Canada, and subsequent reports of isolation and acquisition of the pathogen occurred worldwide (Li et al., 2017b). At present, there are no effective vaccines and drugs to prevent and control the disease (Lv et al., 2017). Therefore, researches on the pathogenesis of PHEV and the development of antiviral drugs have become the focus of current research.

Recent studies have shown that dynamic reorganization of the actin cytoskeleton is essential for viral entry, intracellular trafficking, and virion release (Spear and Wu, 2014). The virus has evolved a series of mechanisms to hijack cellular signaling pathways that regulate actin dynamics for efficient infection (Foo and Chee, 2015). Integrins are located on the cell surface in the form of heterodimers by the alpha and beta subunits (Zheng et al., 2017). It is an important receptor for fibronectin (FN) in the matrix, which mediates the interaction between cells and extracellular matrix proteins, and plays an important role in cell movement, migration, and neural cell remodeling (Wu et al., 2017). Integrins have been implicated to promote the entry of different types of viruses, such as human herpesvirus, Ross River virus (RRV), Human immunodeficiency virus (HIV) (Hussein et al., 2015; Lertjuthaporn et al., 2018; Yang et al., 2016). Upon integrin activation, the virus induces FAK phosphorylation, followed by activation of several related signaling molecules to facilitate entry into host cells, including Src, PI-3 K, Rho GTPases (RhoA, Rac and Cdc42) and other effector molecules such as AKT, PAK, MAPK (MEK, ERK1/2), LIMK, and cofilin (Abban and Meneses, 2010; Bottero et al., 2013; Krishnan et al., 2006). Our previous studies suggested that dynamic changes in the actin cytoskeleton are essential for PHEV entry and integrin α5β1-FAK signaling pathway plays a key role in this process (Lv et al., 2019). Therefore, drugs targeting integrin α5β1 are promising methods for treating PHE.

ATN-161 (Ac-PHSCN-NH2) is a small peptide antagonist of integrin α5β1, a recently developed anticancer drug that interacts with the N-terminus of the β1 region of integrin α5β1 to lock integrin α5β1 in its

* Corresponding author.
E-mail address: gaofeng@jlu.edu.cn (F. Gao).
[1] These authors contributed equally to this article.

https://doi.org/10.1016/j.vetmic.2019.04.029
Received 1 February 2019; Received in revised form 24 April 2019; Accepted 24 April 2019

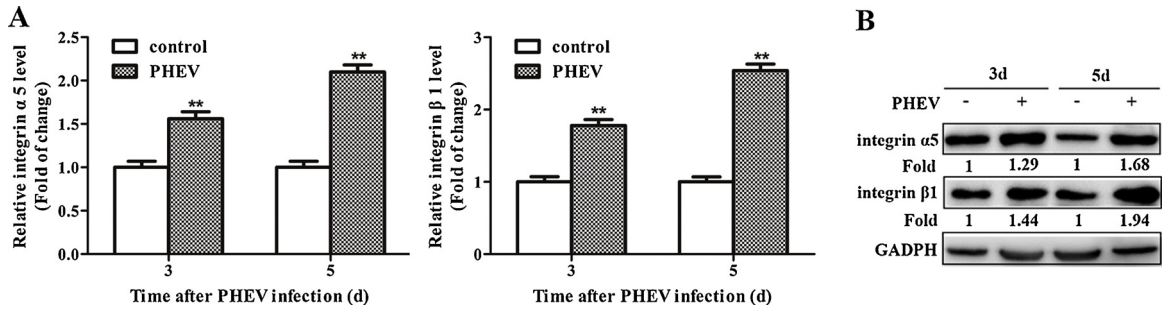

Fig. 1. Expression of integrin α5β1 is increased in PHEV-infected mice. (A) The expression of integrin α5 and integrin β1 in the brain of BALB/c mice at different time points after infection with PHEV ($TCID_{50}$ = $10^{-4.5}$/0.1 mL) was determined by qPCR. (B) Western blotting was performed to examine the expression of integrin α5 and integrin β1 protein in brain tissue of PHEV-infected mice at different time points. All of the data are representative of at least three independent experiments. *P < 0.05, **P < 0.01 vs. normal controls.

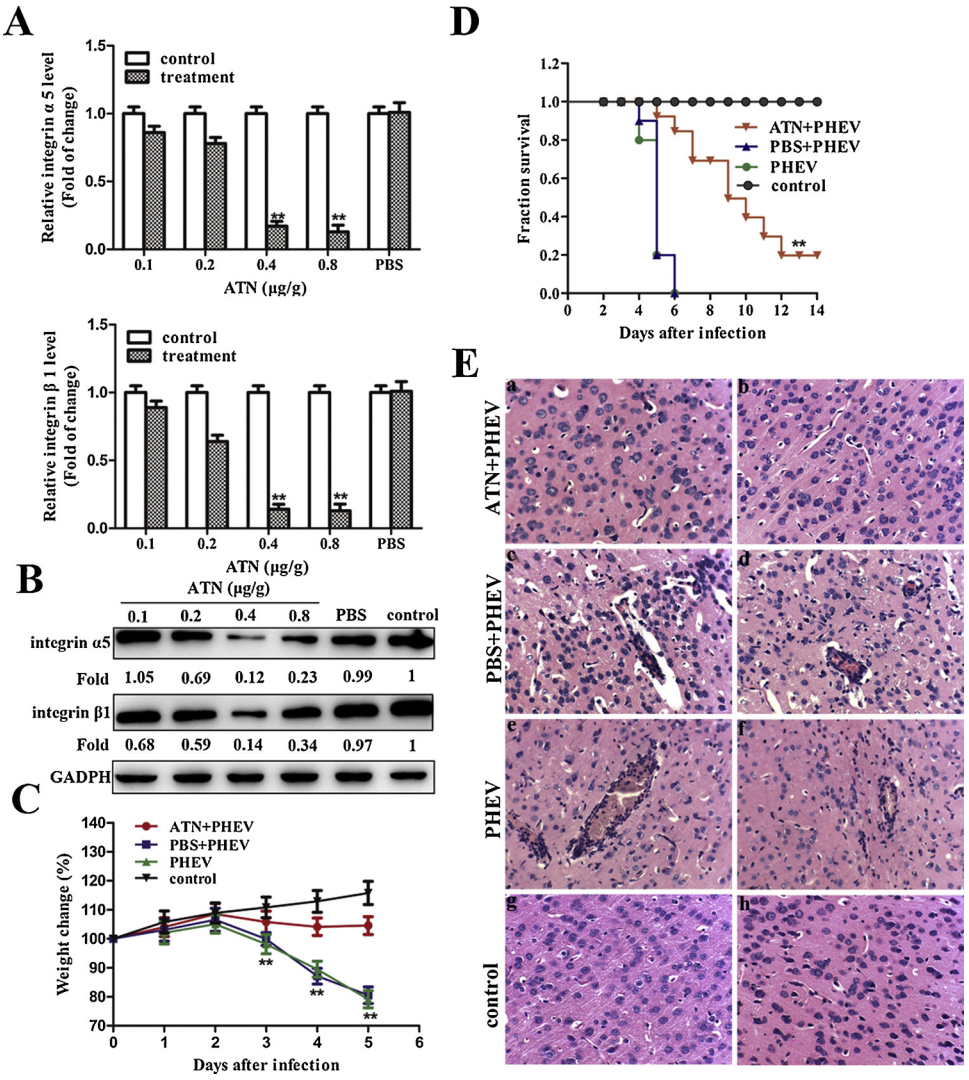

Fig. 2. ATN-161 reduces symptoms in PHEV-infected mice. (A–B) Design and optimize ATN-161 appropriate treatment strategy for PHEV infection. The relative expression levels of integrin α5 and integrin β1 in mouse brain tissue after intravenous injection of different doses of ATN-161 or same volume PBS, were detected by qPCR and Western blotting (n = 3). (C) Mice were intravenously injected with ATN-161, the same volume of PBS, or not treated. At 24 h post injection, the mice were inoculated with PHEV or no treatment. Percentage change in body weight of mice in each group was monitored daily. n = 10 mice per group. (D) The clinical symptoms of the mice as described in (C) were monitored daily, and survival curves were presented at each time point. n = 10 mice per group. (E) Representative sections of brain tissue from each group of mice infected with PHEV for 5 days. H&E staining, ×400. (a–b) The perivascular space widened, a small number of nerve cells showed degeneration and necrosis. (c–f) Perivascular cuff and degeneration and necrosis of many nerve cells. (g–h) Negative control. All of the data are representative of at least three independent experiments. *P < 0.05, **P < 0.01 vs. normal controls.

non-activated conformation (Wang et al., 2016). The drug has been tested in Phase 2 clinical trials and can lead to stable disease in patients with solid tumors (Kaemmerer et al., 2014). However, it is unclear whether ATN-161 has antiviral effects on PHEV. In this study, we demonstrated that ATN-161 had an antiviral effect and explored potential mechanisms of action.

2. Materials and methods

2.1. Virus and PHEV-infected mice model

PHEV 67 N (GenBank accession No. AY078417) was the strain used in this experiment, which was propagated in mouse neuroblastoma (Neuro-2a, N2a) cells. BALB/c mice (3 weeks old) were obtained from the Laboratory Animal Centre, Jilin University. The PHEV-infected model was established in mice, as reported previously (Lan et al.,

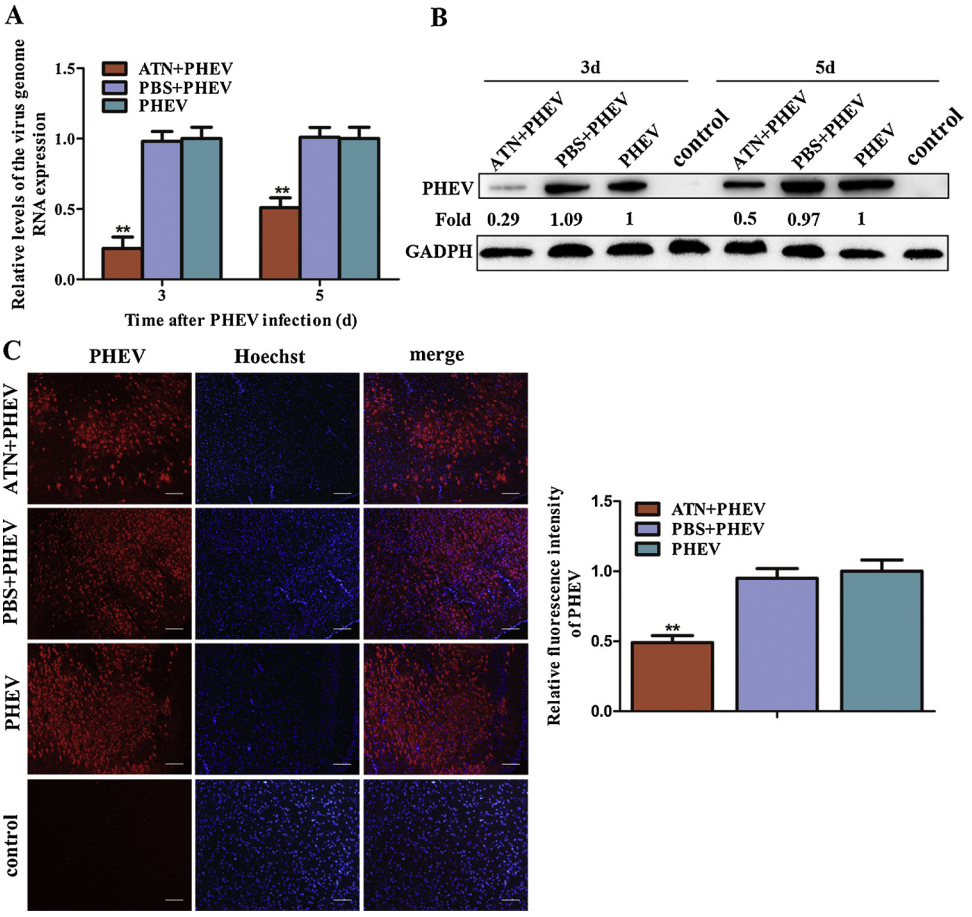

Fig. 3. ATN-161 reduces the expression of virus in PHEV-infected mice brain tissue. (A) Relative expression of viral RNA in brain tissue at different time points after treatment was detected by qPCR. (B) Expression of PHEV protein in brain tissue at different time points after treatment was determined by Western blotting. (C) Indirect immunofluorescence was performed to examine the expression of PHEV in brain tissue of mice of each group 5 days after treatment and observed by confocal microscopy. PHEV-positive neurons were labeled with an anti-S protein monoclonal antibody (red) and the nuclei were marked with hoechst (blue). Quantitative analysis is summarized in the histograms on the right. Five representative fields were counted in each experiment. Scale bar = 10 μm. All of the data are representative of at least three independent experiments. *P < 0.05, **P < 0.01 vs. normal controls (For interpretation of the references to colour in this figure legend, the reader is referred to the web version of this article).

2014).

2.2. Reagents

ATN-161 was purchased from Selleck (Houston, Texas, USA). Integrin α5 (D7B7G) Rabbit mAb, Integrin β1 (D6S1W) Rabbit mAb, FAK (D2R2E) Rabbit mAb, Phospho-FAK (Tyr576/577) Antibody, Rac1/Cdc42 Antibody, Cofilin (D3F9) XP® Rabbit mAb (CFL) and Phospho-Cofilin (Ser3) (77G2) Rabbit mAb (p-CFL) were purchased from Cell Signaling Technology (Beverly, MA). LIM Kinase 1 Polyclonal Antibody and and phospho-LIM Kinase 1 (Thr508) were purchased from BIOSS (Beijing, China). GAPDH antibody, horseradish peroxidase-linked secondary anti-rabbit or anti-mouse IgG antibodies, (Cy3)-conjugated Affinipure Goat Anti-Mouse IgG (H + L) secondary antibodies, and ECL detection kit were purchased from Proteintech (Chicago, USA). Mouse anti-PHEV-S antibody was a laboratory prepared monoclonal antibody.

2.3. Animal protocols

The ATN-161 used in this study is a small peptide antagonist that binds to integrin α5β1. The mice were injected intravenously with 0, 0.1, 0.2, 0.4, and 0.8 μg/g of ATN-161, respectively. Brain tissue was collected at 24 h after injection to detect the expression levels of integrin α5 and integrin β1.

The optimal concentration of ATN-161 was screened by the above method, and the mice were randomly divided into 4 groups of 10 mice each. The groups were as follows: group 1 is ATN-161 and PHEV-infected treatment group (ATN + PHEV); group 2 is phosphate buffer saline (PBS) treatment and PHEV-infected group (PBS + PHEV); Group 3 is the PHEV infection group (PHEV); Group 4 is a blank control group. The mice in the ATN + PHEV group were intravenously injected with optimal concentration of ATN-161. The mice in the other groups were injected with the same volume of control solution or not. Except for the control group, mice of the other groups were intranasally inoculated with 100 μL of PHEV solution ($TCID_{50} = 10^{-4.5}$/0.1 mL) at 24 h after the injection. Mice were sacrificed at different time points, and brain tissues of each group of mice were dissected for the following study. At the same time, parallel experiments were performed to calculate the survival rate of each group of mice.

2.4. RNA extraction and real-time quantitative PCR detecting system (qPCR)

Total RNA from brain tissue of each group of mice in the experiment was extracted using TRIzol Reagent (Invitrogen, Gaithersburg, MD) according to the manufacturer's instructions. The cDNA was generated by reverse transcription using PrimeScript reverse transcriptase (Takara, Janpa). The integrin α5, integrin β1, and viral spike protein genes were detected by qPCR on a CFX96 Touch real-time PCR detection system (Bio-Rad, USA) using TaKaRa SYBR Green qPCR kit (TaKaRa, Japan). GADPH was used as a loading control. The relative expression was analyzed using the $2^{-\triangle\triangle CT}$ method. Primer sequences were as follow: integrin α5 sense primer, 5′- GGC TCC AGG GAG GAG TTC TA -3′; anti-sense primer, 5′- CTT GGC CCA GAC TCG GAA AT -3′; integrin β1 sense primer, 5′- AGC GAT GAG GCT ATT CCG ACT A -3′; anti-sense primer, 5′- AGC GAT GAG GCT ATT CCG ACT A -3′; PHEV sense primer, 5′- GGT ATC AAA GTG TTG CCT CC -3′; anti-sense primer, 5′- GAA CCC TTC CTG GA TAG AAT -3′; mouse GAPDH sense primer, 5′- CTC AAC TAC ATG GTC TAC ATG TTC -3′; anti-sense primer, 5′- ATT TGA TGT TAG TGG GGT CTC GCT C -3′.

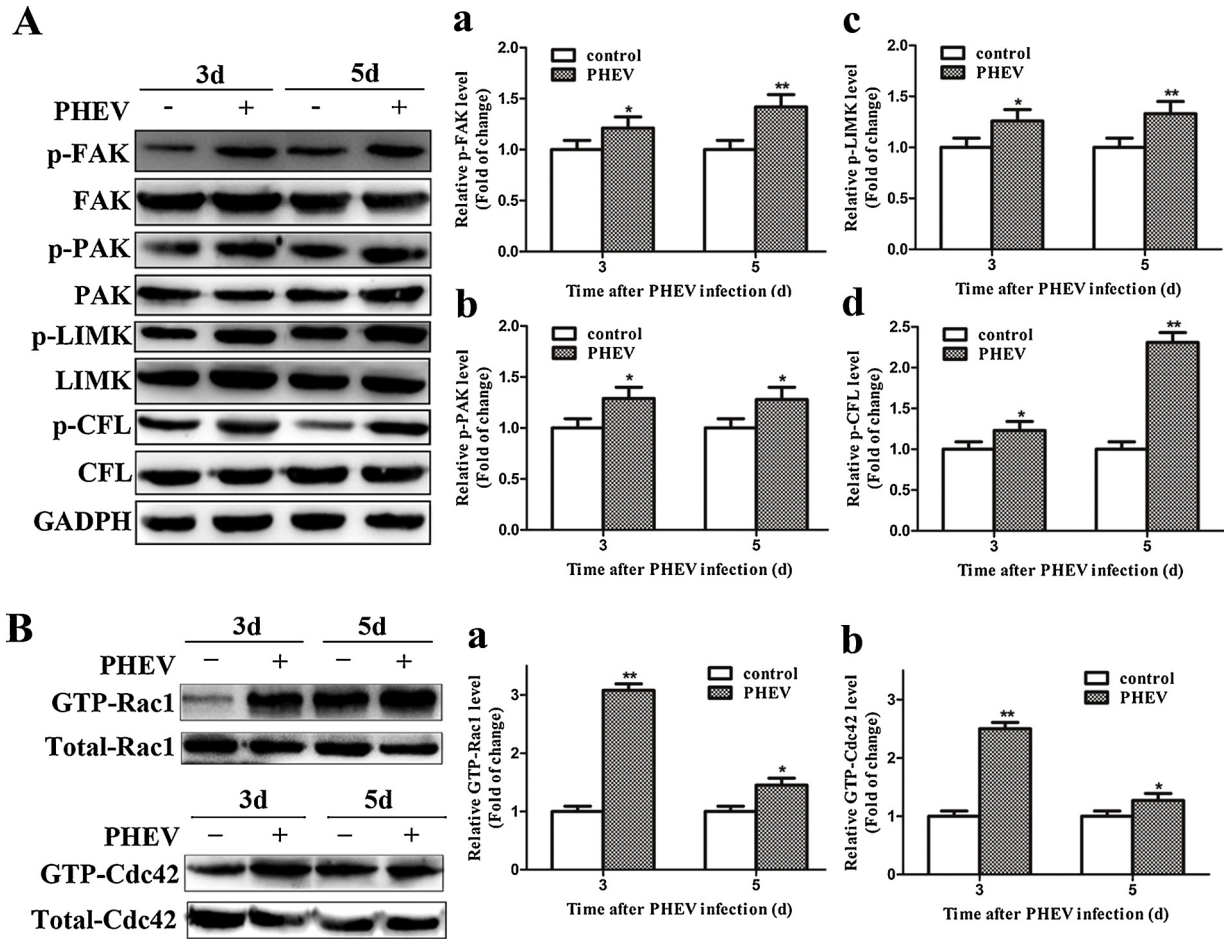

Fig. 4. Integrin α5β1-FAK pathway was activated in PHEV-infected mice. (A) Expression of FAK, p-FAK, PAK, p-PAK, LIMK, p-LIMK, CFL, p-CFL in BALB/c mice at different time points after PHEV infection by Western blotting assay. (a–d) Graph showing p-FAK, p-PAK, p-LIMK, and p-CFL relative protein levels normalized to FAK, PAK, LIMK, and CFL. (B) Rac1 and Cdc42 activation assay. Brain tissue of BALB/c mice at different time points after PHEV infection was collected and lysed, and pull-down assays were performed as described in the material method. (a–b) Graph showing GTP-Rac1 and GTP-Cdc42 relative protein levels normalized to Rac1 and Cdc42. All of the data are representative of at least three independent experiments. *P < 0.05, **P < 0.01 vs. normal controls.

2.5. Western blotting

The brain tissues were washed once with PBS and grinded in liquid nitrogen, followed by lysis using a Radio Immunoprecipitation Assay (RIPA) Lysis Buffer (1% Triton X-100 and 1 mM phenylmethylsulfonyl fluoride [PMSF] in PBS) on ice for 30 min. The protein samples (50 mg/lane) were loaded to 12% sodium dodecyl sulfate (SDS) polyacrylamide gel electrophoresis and were transferred to 0.22 μm polyvinylidene fluoride membranes using the Bio-Rad wet transfer system. Then the membranes were blocked with 5% skim milk powder in PBS for 1 h at 37 °C. After washing with PBS, the membrane was probed with antibodies against indicated primary antibodies at 4 °C overnight. Next, the membranes were washed with PBS containing Tween-20 (PBST) for four times and incubated with horseradish peroxidase-linked secondary anti-rabbit or anti-mouse IgG antibodies for 1 h at 37 °C. After washing with PBST, the signal was visualized using an ECL detection kit. GADPH was used as a loading control.

2.6. GST pull-down assay

The Rac1 and Cdc42 binding domains (PBDs) of PAK1 were first cloned into a plasmid encoding the fusion protein GST-PBD. Expression and purification of GST-PBD protein as previously described (Lv et al., 2019). Subsequently, the GST-PBD protein was incubated with glutathione sepharose 4B beads (catalog number 17075601; GE Healthcare) overnight at 4 °C. The beads were washed for three times with PBS. Brain tissues lysates were centrifuged at 120,000 r/min for 15 min at 4 °C. The supernatant was mixed with glutathione sepharose 4B beads bound to the GST-PBD protein and incubated overnight at 4 °C on a rotary mixer. After washing three times, the lysis buffer and the corresponding volume of 5 × loading buffer were added into the ependorf tube and boiled for 10 min, followed by detection of the target protein by Western blotting.

2.7. Histological analysis

Each group of mice was sacrificed by bleeding and perfused with 4% paraformaldehyde. Brain tissues of each group were embedded in paraffin and 3 μm various sections were prepared and stained with hematoxylin and eosin (H&E). H&E staining was used to evaluate virus-induced neuropathology. The tissue sections were deparaffinized in xylene and then passed through a gradient of ethanol and finally into distilled water. The treated sections were placed in an aqueous solution of hematoxylin for 10 min to stain the nucleus. The sections were then transferred to a staining tank with tap water until the water became clear. The sections were sequentially transferred to a jar containing 70% ethanol for 2 min, 80% ethanol for 2 min, 90% ethanol for 2 min, 95% ethanol for 2 min, and 100% ethanol for 1 min. Sections were transferred to Eosin solution for 3 min then 80% ethanol for 10 s, 90% ethanol for 10 s, 95% ethanol for 10 s, 100% ethanol for 1 min, and xylene for 5 min. The sections were removed from the xylene and placed in a fume hood until the slides were dry. The sections were

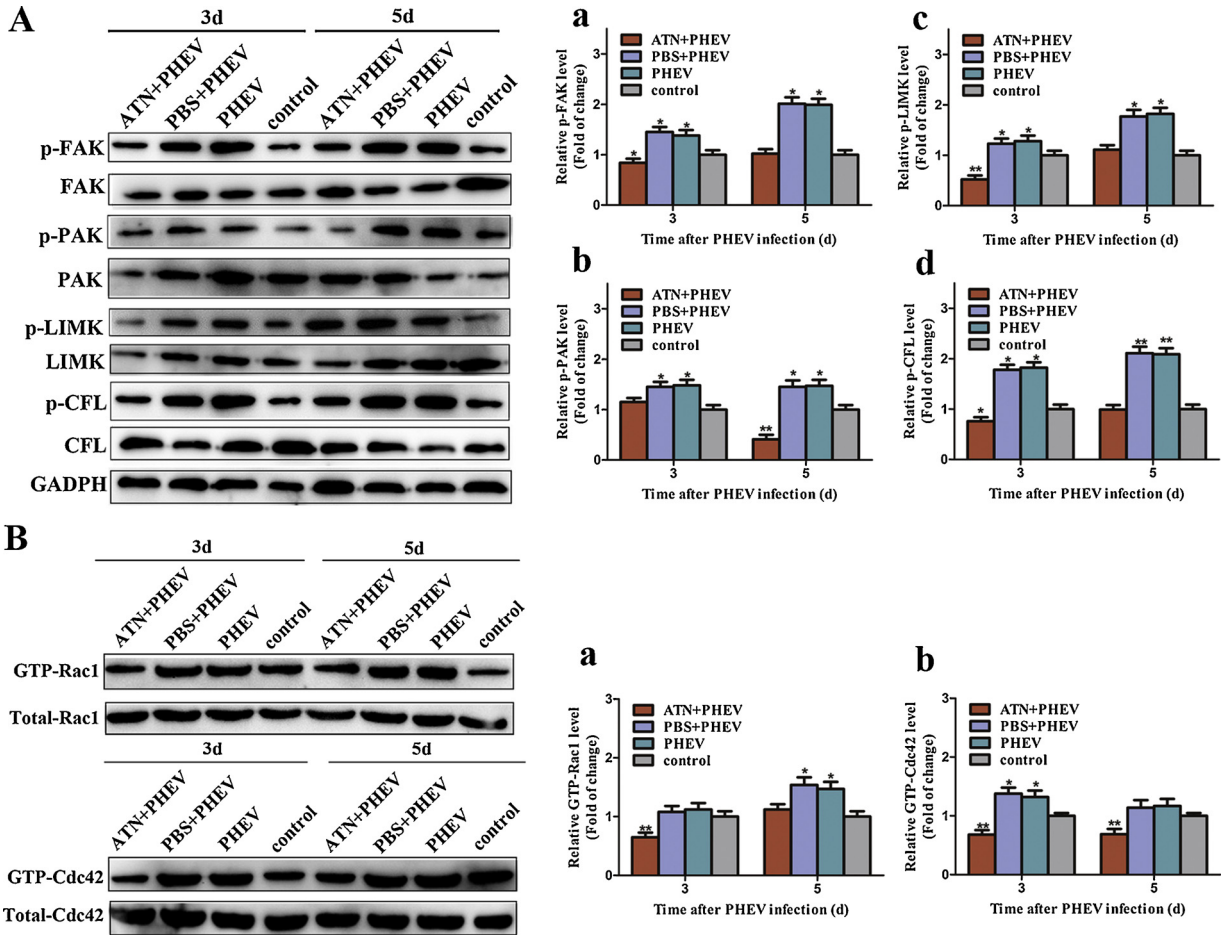

Fig. 5. ATN-161 reduces integrin α5β1-FAK pathway activation in PHEV-infected mice. (A) Western blotting was performed to examine integrin α5β1-FAK pathway activation in the brain tissue of mice of each group in 5 days after treatment. (a–d) Graph showing p-FAK, p-PAK, p-LIMK, p-CFL relative protein levels normalized to FAK, PAK, LIMK, and CFL. (B) Rac1 and Cdc42 activation assay. Brain tissue of each group of mice 5 days after PHEV infection was collected and lysed, and pull-down assays were performed as described above. (a–b) Graph showing GTP-Rac1 and GTP-Cdc42 relative protein levels normalized to Rac1 and Cdc42. All of the data are representative of at least three independent experiments. *P < 0.05, **P < 0.01 vs. normal controls.

sealed with neutral gum and stored at room temperature. Capture images of hematoxylin and eosin stained with a 14.0 M P digital microscope camera.

2.8. Indirect immunofluorescence

Each group of mice was sacrificed at different time points by bleeding, and the brain tissues were cut into frozen-sections. Sections were fixed with 4% paraformaldehyde for 15 min at room temperature and then permeabilized with 0.1% Triton X-100 and blocked with 5% non-fat milk powder for 1 h at 37 °C, then wash with PBS and incubate overnight at 4 °C with PHEV monoclonal antibody. After washing with PBS, (Cy3)-conjugated Afflnlpure goat anti-mouse IgG (H + L) secondary antibody was incubated for 1 h at 37 °C. Hoechst was used to stain the nucleus. After washing with PBS, the coverslips were fixed on glass with an anti-fluorescent attenuating mount and then observed on a cofocal microscope.

2.9. Statistical analysis

Values are presented as an arithmetic mean ± standard error. All data were analyzed by SPSS 17.0 software (Chicago, USA). Histogram was carried out with GraphPad Prism 5.0 software (San Diego, USA). Western blotting pictures were analyzed by Tanon Gis software (Shang Hai, China). Fluorescence intensity was analyzed by ImageJ software (National Institutes of Health, USA). All results were considered statistically significant at the p values < 0.05 level.

3. Results

3.1. Expression of integrin α5β1 is increased in PHEV-infected mice

In our previous study, we found that integrin α5β1 expression was increased in PHEV-infected N2a cells and was essential for viral entry and proliferation. To determine if integrin α5β1 has similar functions in vivo, we established a mouse infection model to detect integrin α5β1 expression in vivo after PHEV infection. At 3 day post-infection (dpi), the appetite of the mice decreased and the weight loss rate increased. At 5 dpi, the mice developed typical neurological symptoms, including systemic muscle tremor, hyperesthesia, standing, etc. Therefore, the brain tissue of mice collected at these two time points was studied. qPCR and Western blotting results showed that the expression of integrin α5β1 was up-regulated in the brain tissue of PHEV-infected mice (Fig.1 A and B). These results indicate that integrin α5β1 may play a role in viral infection in vivo.

3.2. Integrin α5β1 inhibitor ATN-161 reduces symptoms in PHEV-infected mice

To confirm whether integrin α5β1 affects PHEV proliferation in vivo, we performed the following experiment. BALB/c mice were injected intravenously with ATN-161 at 2 day intervals, following a

design concentration gradient (0, 0.1, 0.2, 0.4 and 0.8 μg/g) to determine the lowest effective dose in mouse brain tissue. After three injections, brain tissue was collected at 24 h after injection to detect the expression levels of integrin α5 and integrin β1. The analysis of qPCR and Western blotting results revealed that ATN-161 significantly reduced the expression of integrin α5β1 at concentrations of 0.4 and 0.8 μg/g and there was no significant difference between the two concentrations (Fig.2 A and B). Therefore, we chose 0.4 μg/g as an optimal dose used for subsequent experiments.

The mice were intravenously injected with ATN-161 (0.4 μg/g) or PBS (same volume), and the PHEV nasal cavity was inoculated at 24 h after the injection. At 5 dpi, the weight of the control mice increased steadily, increasing to 115% of their origination, and that increase was also seen in the ATN + PHEV group mice. In the PBS + PHEV group and the PHEV group, the body weight has dropped to about 80% of the original body weight (Fig. 2C). In addition, at 5 dpi, mice in the PHEV group and the PBS + PHEV group showed typical symptoms of encephalomyelitis, including muscle weakness, convulsions, hunched posture, and hyperesthesia. These typical symptoms did not appear in the ATN + PHEV group. Compared with PBS + PHEV or PHEV group mice, the survival time of ATN-injected mice was significantly extended (Fig. 2D). At 9 dpi, the typical symptoms of encephalomyelitis occurred in the ATN + PHEV group, indicating a significant delay in the course of the disease. All mice in the PHEV group and the PBS + PHEV group died, while two mice in the ATN + PHEV group eventually survived (Fig. 2D). Furthermore, the brain tissue of each group of mice was observed by paraffin section at 5dpi. H&E staining determined that the cerebral cortex of mice in the PBS + PHEV group and the PHEV group showed neuronal shrinkage, cytoplasmic swelling, and perivascular cuff. However, the brain tissue of the ATN + PHEV group did not change significantly compared with the control group (Fig. 2E). Taken together, these results indicated that ATN reduced neurological damage caused by PHEV and delayed the progression of the disease and prolonged mice survival.

3.3. ATN-161 reduces the expression of virus in PHEV-infected mice brain tissue

We used qPCR, Western blotting, and indirect immunofluorescence to determine the effects of the ATN-161 on the viral proliferation after injection. At 3 dpi and 5 dpi, the brain tissue of the mice was collected to detect the virus content. QPCR and Western blotting results showed that the expression of viral RNA and protein in mice brain tissue was down-regulated after injecting with ATN-161 (Fig. 3A and B). Immunofluorescence staining with monoclonal antibodies against PHEV S protein was used. Fluorescence signals at the same position in the cerebral cortex of each group of mice were collected, and the results showed that the number of PHEV-infected neurons in the brain tissue of ATN-161-treated mice was significantly reduced (Fig. 3C).

3.4. Inhibition of integrin α5β1 by ATN-161 reduces FAK pathway activation in PHEV-infected mice

We can confirm that integrin α5β1 is essential for virus proliferation in vivo through the above experiments. PHEV promotes actin cytoskeletal rearrangement by activating the integrin α5β1-FAK-Rac1/Cdc42-PAK-LIMK-Cofilin (CFL) pathway, hence facilitating its own invasion and proliferation in vitro (Lv et al., 2019). To understand the mechanism by which integrin α5β1 affects PHEV proliferation in vivo, we next determined whether FAK signaling pathways was involved. BALB/c mice were intranasally inoculated with PHEV and brain tissue was collected at 3 dpi and 5 dpi. Protein expression of FAK, p-FAK, PAK, p-PAK, LIMK, p-LIMK, CFL, and p-CFL in brain tissue of PHEV-infected mice and control mice were detected by Western blotting assay. The results showed that the expression levels of p-FAK, p-PAK, p-LIMK, and p-CFL protein were increased (Fig. 4A). Rac1 and Cdc42 are members of the Rho family and play a regulatory role by converting the inactive form of GDP binding to the activated form of GTP binding. We detected the activation of Rac1 and Cdc42 by the previously established GST pull-down assay. The results confirmed that Rac1 and Cdc42 were activated during the PHEV infection (Fig. 4B).

In addition, we also tested the activation of integrin α5β1-FAK signaling pathway in brain tissue of ATN-161 injected mice to determine its mechanism of inhibition of viral proliferation. The results showed that the activation of integrin α5β1-FAK-Rac1/Cdc42-PAK-LIMK-CFL signaling pathway in brain tissue of ATN + PHEV group was significantly inhibited compared with that of PBS + PHEV group and PHEV group (Fig.5A and B). Therefore, ATN-161 reduces the proliferation of PHEV in mouse brain tissue by inhibiting the activation of integrin α5β1-FAK-Rac1/Cdc42-PAK-LIMK-CFL pathway.

4. Discussion

Integrins are members of a family of cell adhesion molecules that provide a link between extracellular matrix (ECM) proteins and actin cytoskeletal proteins, essential for regulating cytoskeleton and intracellular signaling pathways, which are all essential for cell survival, proliferation, shape necessities, attachment, migration, and angiogenesis (Parolin et al., 2018). Approximately 24 integrins have been identified. These heterodimeric receptor molecules are derived from different pairs between the 18a and 8b subunits (Niu and Li, 2017). With the role of integrin in cerebrovascular diseases has been proposed, it is closely related to multiple stages of neurodevelopment and a variety of neuropathological processes (Sun et al., 2017; Welser et al., 2017). Furthermore, many pathogens have the ability to invade cells using integrin with different mechanisms, including viruses and bacteria (Kim et al., 2018; Morris et al., 2018). Virus-integrin binding has been shown to promote adhesion, cytoskeletal rearrangement, integrin activation and increased intracellular signaling (Hussein et al., 2015). HIV-1 interacts with integrin a4b7 via gp120, which is essential for efficient intercellular transmission of the virus (Lertjuthaporn et al., 2018). Therefore, the treatment of targeting integrins has received more and more attention. PHEV is a typical neurotropic virus that can cause extensive neurological damage in infected host animals (Li et al., 2018). In the brain tissue of the mouse infection model, neuronal edema, swelling of the cell body, partial dissolution of the Nissl body, concentration of the neuron nuclei, and severe staining were observed (Lan et al., 2014). Integrin α5β1 is an important member of the integrin family and is essential for angiogenesis, neurological recovery, etc (Lu et al., 2018; Sui et al., 2018). Integrin α5β1 has been shown to be associated with many viral invasion of host cells, such as Human Immunodeficiency Virus (HIV), Ebola virus, Epstein-Barr virus (EBV) (Hussein et al., 2015). Previous studies have demonstrated that PHEV can promote its entry into N2a cells through integrin α5β1 pathway (Lv et al., 2019). But, the role of integrin α5β1 pathway in vivo is not clear.

In this article, we detected that the expression level of integrin α5β1 in PHEV-infected mice and found an increased expression in mice. This was consistent with the results that in vitro (Lv et al., 2019). It is suggested that there was a close relationship between integrin α5β1 and PHEV proliferation in vivo. To further investigate the role of integrin α5β1 in the proliferation of PHEV in vivo, we used ATN-161 to inhibit the expression of integrin α5β1 and analyzed the effect of inhibitor on PHEV proliferation and its therapeutic effect. ATN-161 is a non-RGD-based integrin-binding peptide that targets α5β1. It inhibits the migration and adhesion of specific integrins on activated endothelial cells, which plays a key role in tumor angiogenesis (Wang et al., 2016). However, whether ATN-161 has antiviral effects has not been reported. After ATN-161 treatment of mice, the expression of PHEV in mouse brain decreased by 50%–70%. In addition, ATN-161 treatment delayed the onset of mice, reduced symptoms, decreased weight loss, and significantly prolonged survival. Histological observations showed that the neuronal cells of ATN-161 treated mice tend

to be normal, and there were no typical non-suppurative encephalitis symptoms at 5 dpi. The number of PHEV-positive neurons in ATN-161 treated mice was also significantly reduced by indirect immunofluorescence. The above experiments confirmed that integrin α5β1 promoted PHEV proliferation in vivo and ATN-161 had a certain antiviral effect. This experiment provides a theoretical basis for the development of clinical antiviral drugs targeting integrin α5β1.

We then explored the possible mechanisms by which integrin α5β1 was involved in the PHEV proliferation process. Normally, the virus activates integrin and induces its downstream protein activation to promote its own invasion and proliferation. Human papillomavirus type 16 (HPV16) binds to heparan sulfate and then activates FAK via integrins to promote infection (Abban and Meneses, 2010). Kaposi's sarcoma-associated herpesvirus (KSHV) induces activation of the integrin-dependent FAK-Src-PI-3 K-Rho GTPase kinase pathway. These signaling pathways play an important role in host cell endocytosis and cytoplasmic transport (Kerur et al., 2010). Previous studies have confirmed that PHEV promotes its entry into N2a cells by activating the integrinα5β1-FAK signaling pathway (Lv et al., 2019). Therefore, this study detected whether the signaling pathway was activated in the brain tissue of PHEV-infected mice. Western blotting and GST pull-down results indicated that each molecule of the signaling pathway was activated. The activation of this pathway was inhibited after ATN-161 treatment, suggesting that PHEV also promoted its invasion and proliferation through the integrin α5β1-FAK signaling pathway in vivo.

In conclusion, our study demonstrated that integrin α5β1-FAK signaling pathway participated in PHEV proliferation in a mouse model for the first time. Intravenous injection of ATN-161 to inhibit integrin α5β1 can reduce PHEV expression and has therapeutic effects. Therefore, our results provide a theoretical basis for the clinical application of ATN-161 and other anti-viral drugs targeting integrin α5β1.

Competing interests

The authors declare that they have no conflict of interest.

Acknowledgments

This study was supported by the National Key Research and Development Program of China (grant 2016YFD0500102), the National Natural Science Foundation of China (grants 31872446, 31772704, 31672519, and 31602018), the Scientific and Technological Project of Jilin Province (grants 20180101270JC, and 20170204033NY).

References

Abban, C.Y., Meneses, P.I., 2010. Usage of heparan sulfate, integrins, and FAK in HPV16 infection. Virology 403, 1–16.

Bottero, V., Chakraborty, S., Chandran, B., 2013. Reactive oxygen species are induced by Kaposi's sarcoma-associated herpesvirus early during primary infection of endothelial cells to promote virus entry. J. Virol. 87, 1733–1749.

Foo, K.Y., Chee, H.Y., 2015. Interaction between flavivirus and cytoskeleton during virus replication. Biomed. Res. Int. 2015, 427814.

Hussein, H.A., Walker, L.R., Abdel-Raouf, U.M., Desouky, S.A., Montasser, A.K., Akula, S.M., 2015. Beyond RGD: virus interactions with integrins. Arch. Virol. 160, 2669–2681.

Kaemmerer, E., Melchels, F.P., Holzapfel, B.M., Meckel, T., Hutmacher, D.W., Loessner, D., 2014. Gelatine methacrylamide-based hydrogels: an alternative three-dimensional cancer cell culture system. Acta Biomater. 10, 2551–2562.

Kerur, N., Veettil, M.V., Sharma-Walia, N., Sadagopan, S., Bottero, V., Paul, A.G., Chandran, B., 2010. Characterization of entry and infection of monocytic THP-1 cells by Kaposi's sarcoma associated herpesvirus (KSHV): role of heparan sulfate, DC-SIGN, integrins and signaling. Virology 406, 103–116.

Kim, Y.R., Byun, M.R., Choi, J.W., 2018. Integrin alpha6 as an invasiveness marker for hepatitis B viral X-driven hepatocellular carcinoma. Cancer Biomark. 23, 135–144.

Krishnan, H.H., Sharma-Walia, N., Streblow, D.N., Naranatt, P.P., Chandran, B., 2006. Focal adhesion kinase is critical for entry of Kaposi's sarcoma-associated herpesvirus into target cells. J. Virol. 80, 1167–1180.

Lan, Y., Zhao, K., Zhao, J., Lv, X., Wang, G., Lu, H., Tang, B., Li, Z., Chang, L., Jin, Z., He, W., Gao, F., 2014. Gene-expression patterns in the cerebral cortex of mice infected with porcine haemagglutinating encephalomyelitis virus detected using microarray. J. Gen. Virol. 95, 2192–2203.

Lertjuthaporn, S., Cicala, C., Van Ryk, D., Liu, M., Yolitz, J., Wei, D., Nawaz, F., Doyle, A., Horowitch, B., Park, C., Lu, S., Lou, Y., Wang, S., Pan, R., Jiang, X., Villinger, F., Byrareddy, S.N., Santangelo, P.J., Morris, L., Wibmer, C.K., Biris, K., Mason, R.D., Gorman, J., Hiatt, J., Martinelli, E., Roederer, M., Fujikawa, D., Gorini, G., Franchini, G., Arakelyan, A., Ansari, A.A., Pattanapanyasat, K., Kong, X.P., Fauci, A.S., Arthos, J., 2018. Select gp120 V2 domain specific antibodies derived from HIV and SIV infection and vaccination inhibit gp120 binding to alpha4beta7. PLoS Pathog. 14, e1007278.

Li, Z., He, W., Lan, Y., Zhao, K., Lv, X., Lu, H., Ding, N., Zhang, J., Shi, J., Shan, C., Gao, F., 2016. The evidence of porcine hemagglutinating encephalomyelitis virus induced nonsuppurative encephalitis as the cause of death in piglets. Peer J. 4, e2443.

Li, Z., Zhao, K., Lan, Y., Lv, X., Hu, S., Guan, J., Lu, H., Zhang, J., Shi, J., Yang, Y., Song, D., Gao, F., He, W., 2017a. Porcine hemagglutinating encephalomyelitis virus enters Neuro-2a cells via clathrin-mediated endocytosis in a Rab5-, cholesterol-, and pH-Dependent manner. J. Virol. 91, e01083–01017.

Li, Z., Lan, Y., Zhao, K., Lv, X., Ding, N., Lu, H., Zhang, J., Yue, H., Shi, J., Song, D., Gao, F., He, W., 2017b. miR-142-5p disrupts neuronal morphogenesis underlying porcine hemagglutinating encephalomyelitis virus infection by targeting Ulk1. Front. Cell. Infect. Microbiol. 7, 155.

Li, Z., Zhao, K., Lv, X., Lan, Y., Hu, S., Shi, J., Guan, J., Yang, Y., Lu, H., He, H., Gao, F., He, W., 2018. Ulk1 governs nerve growth Factor/TrkA signaling by mediating Rab5 GTPase activation in porcine hemagglutinating encephalomyelitis virus-induced neurodegenerative disorders. J. Virol. 92.

Lu, M., Zhuang, X., Tang, K., Wu, P., Guo, X., Yin, L., Cao, H., Zou, D., 2018. Intrinsic surface effects of tantalum and titanium on integrin alpha5beta1/ ERK1/2 pathway-mediated osteogenic differentiation in rat bone mesenchymal stromal cells. Cell. Physiol. Biochem. 51, 589–609.

Lv, X., Zhao, K., Lan, Y., Li, Z., Ding, N., Su, J., Lu, H., Song, D., Gao, F., He, W., 2017. miR-21a-5p contributes to porcine hemagglutinating encephalomyelitis virus proliferation via targeting CASK-Interactive Protein1 in vivo and vitro. Front. Microbiol. 8, 304.

Lv, X., Li, Z., Guan, J., Hu, S., Zhang, J., Lan, Y., Zhao, K., Lu, H., Song, D., He, H., Gao, F., He, W., 2019. Porcine hemagglutinating encephalomyelitis virus activation of the integrin α5β1-FAK-Cofilin pathway causes cytoskeletal rearrangement to promote its invasion of N2a cells. J. Virol. 93.

Morris, M.A., Laverick, L., Wei, W., Davis, A.M., O'Neill, S., Wood, L., Wright, J., Dawson, C.W., Young, L.S., 2018. The EBV-Encoded oncoprotein, LMP1, induces an epithelial-to-Mesenchymal transition (EMT) via its CTAR1 domain through integrin-mediated ERK-MAPK signalling. Cancers (Basel) 10.

Niu, J., Li, Z., 2017. The roles of integrin alphavbeta6 in cancer. Cancer Lett. 403, 128–137.

Parolin, C., Frisco, G., Foschi, C., Giordani, B., Salvo, M., Vitali, B., Marangoni, A., Calonghi, N., 2018. Lactobacillus crispatus BC5 interferes with Chlamydia trachomatis infectivity through integrin modulation in cervical cells. Front. Microbiol. 9, 2630.

Shi, J., Zhao, K., Lu, H., Li, Z., Lv, X., Lan, Y., Guan, J., He, W., Gao, F., 2018. Genomic characterization and pathogenicity of a porcine hemagglutinating encephalomyelitis virus strain isolated in China. Virus Genes 54, 672–683.

Spear, M., Wu, Y., 2014. Viral exploitation of actin: force-generation and scaffolding functions in viral infection. Virol. Sin. 29, 139–147.

Sui, A., Zhong, Y., Demetriades, A.M., Lu, Q., Cai, Y., Gao, Y., Zhu, Y., Shen, X., Xie, B., 2018. Inhibition of integrin alpha5beta1 ameliorates VEGF-induced retinal neovascularization and leakage by suppressing NLRP3 inflammasome signaling in a mouse model. Graefes Arch. Clin. Exp. Ophthalmol. 256, 951–961.

Sun, J., Yu, L., Huang, S., Lai, X., Milner, R., Li, L., 2017. Vascular expression of angiopoietin1, alpha5beta1 integrin and tight junction proteins is tightly regulated during vascular remodeling in the post-ischemic brain. Neuroscience 362, 248–256.

Wang, W.Q., Wang, F.H., Qin, W.X., Liu, H.Y., Lu, B., Chung, C., Zhu, J., Gu, Q., Shi, W., Wen, C., Wu, F., Zhang, K., Sun, X.D., 2016. Joint antiangiogenic effect of ATN-161 and Anti-VEGF antibody in a rat model of early wet age-related macular degeneration. Mol. Pharm. 13, 2881–2890.

Welser, J.V., Halder, S.K., Kant, R., Boroujerdi, A., Milner, R., 2017. Endothelial alpha6beta4 integrin protects during experimental autoimmune encephalomyelitis-induced neuroinflammation by maintaining vascular integrity and tight junction protein expression. J. Neuroinflamm. 14, 217.

Wu, X., Muthuchamy, M., Reddy, D.S., 2017. Atomic force microscopy investigations of fibronectin and α5β1-integrin signaling in neuroplasticity and seizure susceptibility in experimental epilepsy. Epilepsy Res. 138, 71–80.

Yang, E., Arvin, A.M., Oliver, S.L., 2016. Role for the alphaV integrin subunit in varicella-zoster virus-mediated fusion and infection. J. Virol. 90, 7567–7578.

Zheng, X., Liu, W., Xiang, J., Liu, P., Ke, M., Wang, B., Wu, R., Lv, Y., 2017. Collagen I promotes hepatocellular carcinoma cell proliferation by regulating integrin β1/FAK signaling pathway in nonalcoholic fatty liver. Oncotarget 8.